Predictions of the Joule-Thomson Inversion Curve for Water and Methanol from the LJ-SAFT EOS

Maghari, Ali*[+]***; Safaei, Zahra***

Department of Physical Chemistry, School of Chemistry, University of Tehran, Tehran, I.R. IRAN

ABSTRACT: *In this work, we have calculated the Joule-Thomson inversion curve of two important associating fluids, namely water and methanol, from the SAFT equation of state. Comparisons with the available experimental data, for water and methanol indicate that this molecular based equation of state gives good prediction of the low temperature branch; but, unfortunately, due to lack of isenthalpic data for high-pressure-high- temperature gas condensate for water and methanol, the reliability of model predictions could not be completely verified. We have also reported the influence of the molecular dipole moment and the segment number on the Joule-Thomson inversion curve.*

KEY WORDS: *Joule-Thomson, Inversion curve, SAFT EOS, Water, Methanol.*

INTRODUCTION

The Joule-Thomson process is commonly used to cool or liquefy gases and its coefficient is the indicator of whether the throttling process produces cooling or heating. The *Joule-Thomson* coefficient is defined as the isenthalpic pressure variations in a real gas cause temperature variations:

$$\mu_{JT} \equiv \left(\frac{\partial T}{\partial p}\right)_H \qquad (1)$$

or equivalently, from the standard thermodynamic relations

$$\mu_{JT} = -\frac{1}{C_p}\left(\frac{\partial H}{\partial p}\right)_T \qquad (2)$$

where C_p is the isobaric heat capacity. Depending on state conditions, μ_{JT} may be positive, negative or zero. If μ_{JT} is positive, reduction in pressure causes reduction in temperature. This will happen at lower initial pressures. If the coefficient is negative, then reduction in pressure causes increase the temperature and we would expect this to happen if the initial pressure is high. Therefore, temperature increases with increasing pressure for an isenthalpic process, reaches a maximum point and then starts to decrease with increasing pressure. The temperature corresponding to this maximum point is called the “inversion point”. The "inversion curve" is the locus of these inversion points on a p-T graph.

Several studies have been performed to predict the *Joule-Thomson* inversion curve (JTIC). Corner [1] was one of the first to calculate inversion curves using equations of state (EOS). Many years later, *Gunn et al*. [2] suggested that it is an extremely severe test of an equation of state and derived a general correlation for simple fluids by

* *To whom correspondence should be addressed.*
+ *E-mail: maghari@khayam.ut.ac.ir*
1021-9986/07/4/69 6/$/2.60

a curve fit to experimental data. Miller [3] calculated the inversion curves for the generalized *Redlich-Kwong* and *Martin* EOSs. *Juris* and *Wenzel* [4] have also studied the JTIC for the virial, *Berthelot*, *Beattie-Bridgeman*, *Benedict-Webb-Rubin*, *Redlich-Kwong* and *Martin-Hou* EOSs. Some other cubic EOSs were tested to predict the JTIC [5-7]. *Maghari* and *Matin* [8] shown that a generalized *van der Waals* EOS, called Deiters EOS, provided the most prediction of the JTIC in the sensitive region. *Chacin et al*. [9] proposed a molecular dynamics procedure for determining the inversion curve of simulated model fluids. *Vrabec et al.* have recently predicted the *Joule-Thomson* inversion curves of 15 simple fluids and refrigerants by molecular simulation [10]. Recently, a molecular based EOS, the Soft-SAFT equation, was used to predict JTIC for carbon dioxide and the n-alkane series [11].Since the prediction of the *Joule-Thomson* inversion curve is known as a severe test of the equation of state, we investigate the performance of a different version of SAFT, called the LJ-SAFT EOS, which was developed by *Kraska* and *Gubbins* [16], for the prediction of most important derivative properties, i.e. *Joule-Thomson* inversion behavior, of two important associating fluids, namely water and methanol.

EQUATION OF STATE

Within the statistical associating fluid theory (SAFT) framework, following the *Wertheim's* theory [12-15], the residual *Helmholtz* energy for a fluid of associating chain molecules is written as a sum of the separate contributions to the *Helmholtz* energy

$$A^{res} \equiv A - A^{ideal} = A^{seg} + A^{chain} + A^{dd} + A^{assoc} \quad (3)$$

where A and A^{ideal} are the total *Helmholtz* energy and the ideal gas *Helmholtz* energy at the same temperature and density, A^{seg} is the *Helmholtz* energy due to segment-segment interactions, A^{chain} is the contribution due to the formation of a chain of m monomers, A^{dd} is the *Helmholtz* energy due to the dipole-dipole interaction and possible induction interactions, and A^{assoc} is the incremental *Helmholtz* energy due to association.

In this ork, the JTIC of water and methanol have been calculated with the LJ-SAFT EOS of *Gubbins* and co-workers [16,17] which has a *Lennard-Jones* term to account for monomer dispersion and overlap interactions.

Segment term

We used the segment term as the LJ-SAFT segment model:

$$A_{LJ}^{seg} = m[A^{hs} + \exp(-\gamma\rho^{*2})\rho^{*}T\Delta B_{2,hBH} + \sum_{i,j} C_{ij} T^{i/2}\rho^{*j}] \quad (4)$$

where

$$A^{hs} = Nk_BT\left[\frac{5}{3}\ln(1-\eta) + \frac{\eta(34-33\eta+4\eta^2)}{6(1-\eta)^2}\right] \quad (5)$$

$$\Delta B_{2,hBH} = \sum_{i=-7}^{0} C_i T^{i/2} \quad (6)$$

$$\rho^{*} = m\rho N\sigma^3 \quad (7)$$

$$\eta = \frac{\pi}{6}\rho^{*}\sigma_{BH}^3 \quad (8)$$

$$\sigma_{BH} = \sum_{k=-2}^{1} D_k T^{k/2} + D_{ln}\ln T \quad (9)$$

where m is the segment number, σ is the scaling distance parameter, k_B is the *Boltzmann's* constant, N is *Avogadro's* number, γis a constant parameter equal to 1.9291, C_i and D_k, C_{ij} and D_{ln} are numerical constants and adjustable parameters, respectively; hBH stands for hybrid *Barker-Henderson*, and details were given by *Kolafa* and *Nezbeda* [18].

Chain term

The chain term was independently derived by *Wertheim* [19] and *Chapman et al*. [20] based on the first-order thermodynamic perturbation theory of associating molecules in the limit of a covalent bonding between the monomers. The results for *Lennard-Jones* model is as follows:

$$A_{LJ}^{chain} = Nk_BT(1-m)\ln g^{LJ}(r=\sigma) \quad (10)$$

where $g^{LJ}(r=\sigma)$ is the LJ radial distribution function (RDF) at contact distance, which can be obtained from a correlation function [21]:

$$g^{LJ}(r=\sigma) = \sum_{k=1}^{5}\sum_{l=1}^{5} a_{kl}(\rho^{*})^k T^{*1-l} \quad (11)$$

Dipole-dipole term

The effect of direct electrostatic forces between polar molecules can be approximated by the multi-polar u-expansion [22,23]. Here, only the leading term of the point dipole- point dipole interaction is included. The resulting *Helmholtz* function is:

$$A^{dipole} = N\varepsilon A_2\left[\frac{1}{1-(A_3/A_2)}\right] \tag{12}$$

where

$$A_2 \equiv -\frac{2\pi}{3}\frac{\rho^*\mu^{*4}}{T^*}J^{(6)} \tag{13}$$

$$A_3 \equiv \frac{32\pi^3}{135}\sqrt{\frac{14\pi}{5}}\frac{\rho^{*2}\mu^{*6}}{T^{*2}}K_{222}^{333} \tag{14}$$

$$T^* \equiv \frac{k_B T}{\varepsilon} \tag{15}$$

$$\rho^* = \rho N\sigma^3 \tag{16}$$

$$\mu^* \equiv \frac{1}{(4\pi\varepsilon_0)^{1/2}}\frac{\mu}{\sqrt{m\varepsilon\sigma^3}} \tag{17}$$

where ε is the potential well-depth parameter. The coefficients $J^{(6)}$ and K_{222}^{333} are integrals over two-body and three-body correlation functions for the LJ fluids [22,23], and $\varepsilon_0=8.9\times10^{-12}C^2N^{-1}m^{-2}$ is the electric permittivity.

Association term

The association contribution on the Helmholtz function is based on the first-order thermodynamic perturbation theory of *Wertheim* [12-15]. The expression for the free energy due to association is given by:

$$A^{assoc} = Nk_BT\left\{\frac{M}{2}+\sum_{a=1}^{M}\left(\ln X_a - \frac{X_a}{2}\right)\right\} \tag{18}$$

where X_a is the fraction of molecules not bonded at site a, and M is the number of site per molecule, which is equal to 4 for water and 2 for methanol. The monomer fraction is related to the association strength Δ as follows:

$$X_a = \frac{1}{1+N\sum_b \rho X_b \Delta_{ab}} \tag{19}$$

The association strength is an integral over the radial distribution function of the reference fluid multiplied by the *Mayer* function of the association potential, which was simplified by *Gubbins et al*. [16,24,25]:

$$\Delta = 4\pi K_{assoc}\left[\exp\left(\frac{\varepsilon_{assoc}}{k_B T}\right)-1\right]I(\rho^*,T^*) \tag{20}$$

where K_{assoc} is an adjustable parameter. The integral $I(\rho^*,T^*)$ was evaluated numerically using the accurate values for the LJ radial distribution function obtained from molecular dynamics simulations and fitted as a function of reduced temperature and reduced density [16]:

$$I(\rho^*,T^*) = \frac{1}{3.84\times10^4}\sum_{k=1}^{4}\sum_{l=1}^{4}A_{ij}\rho^{*k}\,T^{*l} \tag{21}$$

$$\rho^* \le 1.25; \quad 0.7 \le T^* \le 6.0$$

CALCULATION OF THE INVERSION CURVE

The inversion curve can be calculated from any equation of state by satisfying the following condition, for which the *Joule-Thomson* coefficient is equal to zero:

$$T^*\left(\frac{\partial p^*}{\partial T^*}\right)_{\rho^*} - \rho^*\left(\frac{\partial p^*}{\partial \rho^*}\right)_{T^*} = 0 \tag{22}$$

where the reduced pressure $p^*\equiv p\sigma^3/\varepsilon$ can be obtained as

$$p^* = \rho^{*2}\left(\frac{\partial A^*}{\partial \rho^*}\right)_{T^*} \tag{23}$$

where the reduced *Helmholtz* energy is defined as:

$$A^* \equiv \frac{A}{N\varepsilon} \tag{24}$$

Values of segment number m, scaling parameters σ and ε/k_B and reduced dipole-moment μ^* are given in table 1.

Solving Eq. (22) simultaneously with our SAFT EOS provides the locus of points for which the *Joule-Thomson* coefficient is zero. The method of calculation is as follows:

Using SAFT EOS, the expression for $(\partial p^*/\partial T^*)_{p^*}$ and $(\partial p^*/\partial p^*)_{T^*}$ are obtained and Eq. (22) can be written as $f(p^*,T^*)=0$. It must be mentioned that the range of

Table 1: Molecular parameters.

substance	m	σ (Å)	ε/k_B (K)	ε_{assoc}/k_B (K)	K_{assoc}	μ*
water	1.000	3.12	222.3	1415.32	67.003	2.46
methanol	1.586	3.48	121.9	2468.99	430.591	2.17

reduced density for which a real value for T* is 1<p*<1.05. Consequently, for any chosen reduced density for which a real value of T* is obtained the reduced inversion temperature T* can be found, and then the reduced inversion pressure p* can be calculated from the EOS. Therefore, the JTIC can be obtained in terms of T* and p*. Moreover, we may write the equation of state as:

$$g\left(T^*, \rho(T^*), p^*\right),$$

then, $dg = \left(\partial g/\partial p^*\right)_{T^*} dp^* + \left(\partial g/\partial T^*\right)_{p^*} dT^* = 0$ gives $\frac{dp^*}{dT^*} = -\frac{\left(\partial g/\partial T^*\right)_{p^*}}{\left(\partial g/\partial p^*\right)_{T^*}}$, which is the maximum of inversion temperature.

RESULTS AND DISCUSSION

We now attempt to check the reliability of the LJ-SAFT model and its molecular parameters (μ,m,σ,ε, k_{assoc}, ε_{assoc}), obtained already by fitting the experimental data for the vapor pressure and saturated liquid volume (see Ref. [17]), for prediction of one of the most important derivative properties, i.e. *Joule-Thomson* inversion curves, of two selected associating fluids, namely water and methane. The results of *Kraska* and *Gubbins* [17] have shown that the LJ-SAFT EOS predicts accurate phase envelope of associating fluids.

Fig. 1 shows the calculated *Joule-Thomson* inversion curves for water and methanol using the LJ-SAFT EOS. Here, the values of reduced temperature T* are plotted against reduced pressure p*. Both upper and lower branches of the inversion curves are calculated and the whole inversion curve plotted. The low-temperature region of the inversion curves for water and methanol is compared with experimental data taken from the NIST Chemistry Web Book [26].

Both upper and lower branches of the inversion curves are calculated and the whole inversion curve plotted. The low-temperature region of the inversion curves for water and methanol is compared with experimental data taken from the NIST Chemistry Web Book [26]. It must be noticed that points below the inversion curve are in the liquid phase and those above are in the gaseous phase. The region inside the inversion curve, where $\mu_{JT}>0$, is called the cooling region, whereas outside, where $\mu_{JT}<0$, is called heating region. All gases approach ideal behavior at high temperature and low pressure, and the isenthalps correspondingly become flat. The shape of the *Joule-Thomson* inversion curve of a fluid at high temperatures is shown to be directly related to its second and third virial coefficients. The intersection with the temperature axis (the low-pressure limit at high temperatures) marks a point where the tangent to the second virial coefficient passes through the origin, i.e. dB/dT=B/T. The agreement between the calculated and experimental data is excellent on the low temperature side. Unfortunately, due to lack of isenthalpic data for high-pressure-high- temperature gas condensate for water and methanol, the reliability of model predictions could not be completely verified. The average absolute error for the lower-pressure isobar is 1.5% for water and 1.2% for methanol.

To check the influence of the molecular parameters used on the inversion results, we have obtained the JTIC of some arbitrary systems with the same LJ-SAFT EOS, but using four different sets of molecular parameters, i.e. reduced dipole moment μ* and segment number m, that are displayed in Figs. 2 and 3.

For water and alkanols with a low carbon number (like CH_3OH), the dipole interactions are expected to be very important. As seen in Fig. 2, the dipole moment parameter has a large effect on both high-temperature-high- pressure and low-temperature-low-pressure branches.

We note that there is an explicit dependence of the JTIC on molecular dipole moment for any polar system, with both maximum inversion temperatures and pressures increasing as the dipole moment increases. Furthermore, from Fig. 3, we observe that the segment number has a

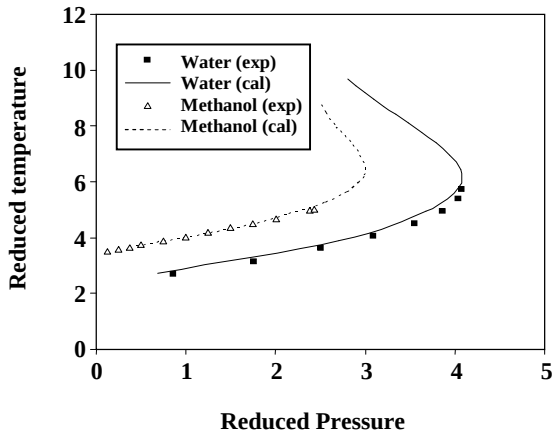

Fig. 1: Calculated JTIC for water and methanol from LJ-SAFT model compared with experimental data. The symbols represent the experimental data taken from NIST [26] and the continuous curves the LJ-SAFT results.

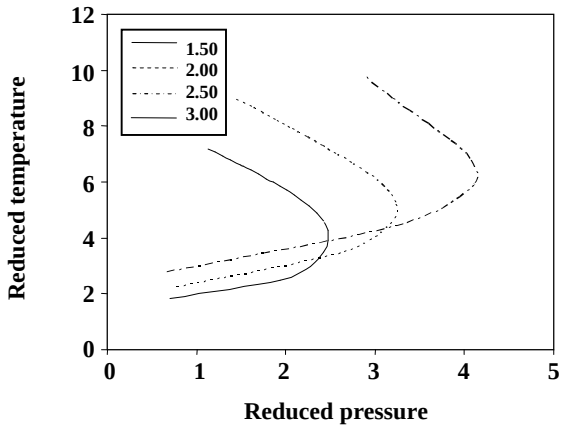

Fig. 2: Calculated JTIC from LJ-SAFT model with different values of reduced dipole moment m^*.

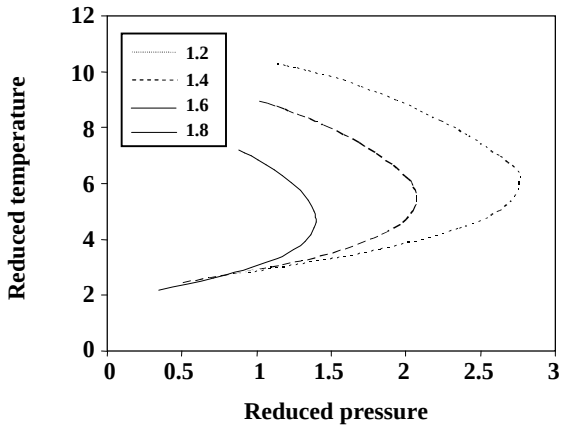

Fig. 3: Calculated JTIC from LJ-SAFT model with different values of segment number m.

large effect on the high-temperature and high-pressure regions, but a small effect on the low-temperature-low-pressure region.

CONCLUSIONS

We have obtained complete *Joule-Thomson* inversion curves for two important associating fluids, including water and methanol, using the LJ-SAFT EOS. Predicted inversion curves were compared with available data. We have observed that the predicted inversion curves strongly depend on the dipole moment and segment number. The dipole moment parameter has a large effect on both high-temperature-high-pressure and low-temperature-low-pressure branches, whereas, the segment number has a large effect on the high-temperature and high-pressure regions, but a small effect on the low-temperature-low-pressure region.

Acknowledgement

We wish to acknowledge the University of Tehran Research Council for the financial support.

Received : 26th August 2006 ; Accepted : 4th December 2006

REFERENCES

[1] Corner, J., *Trans. Farad. Soc*., **35**, 784 (1939).
[2] Gunn, R. D., Chueh, P. L. and Prausnitz, J. M., *Cryogenics*, **6**, 324 (1966).
[3] Miller, D.G., *Ind. Eng. Chem.Fundam*., **9**, 585 (1970).
[4] Juris, K. and Wenzel, L.A., *AIChE J*., **18**, 684 (1972).
[5] Dilay, G.W. and Heidemann, R.A., *Ind. Eng. Chem. Fundam.*, **25**, 152 (1986).
[6] Geneã, D. and Feroiu, V., *Fluid Phase Equilibria*, **77**, 121 (1992).
[7] Matin, N.S. and Haghighi, B., *Fluid Phase Equilibria*, **175**, 273 (2000).
[8] Maghari, A. and Matin, N.S., *J. Chem. Eng. Jpn.*, **30**, 520 (1997).
[9] Chacin, A., Vazquez, J.M. and Muller, E.A., *Fluid Phase Equilibria*, **165**, 147 (1999).
[10] Vrabec, J, Kedia, G.K. and Hasse, H., *Cryogenics*, **45**, 253 (2005).
[11] Colina, C. M., Turrens, L.F., Gubbins, K.E., Fuentes, C.O. and Vega, L.F., *Ind. Eng. Chem. Res*., **41**, 1069 (2002).
[12] Wertheim, M.S, *J. Stat. Phys.*, **35**, 19 (1984).

[13] Wertheim, M.S, *J. Stat. Phys.*, **35**, 35 (1984).
[14] Wertheim, M.S, *J. Stat. Phys.*, **42**, 459 (1984).
[15] Wertheim, M.S, *J. Stat. Phys.*, **42**, 477 (1984).
[16] Müller, E.A. and Gubbins, K.E., *Ind. Eng. Chem. Res*., **34**, 3662 (1995).
[17] Kraska, T. and Gubbins, K.E., *Ind. Eng. Chem. Res*. **35**, 4727 (1996).
[18] Kolafa, J. and Nezbeda, I., *Fluid Phase Equilibria*, **100**, 1 (1994).
[19] Wertheim, M.S., *J. Chem. Phys*., **87**, 7323 (1987).
[20] Chapman, W.G., Jackson, G., and Gubbins, K.E., *Mol. Phys.*, **65**, 1057 (1988).
[21] Johnson, J.K., Müller, E.A. and Gubbins, K.E., *J. Chem. Phys*., **98**, 6413 (1994).
[22] Twu, C.H. and Gubbins, K.E., *Chem. Eng. Sci*., **33**, 863 (1978).
[23] Twu, C.H. and Gubbins, K.E., *Chem. Eng. Sci*., **33**, 879 (1978).
[24] Johnson, J.K. and Gubbins, K.E., *Mol. Phys*. **77**, 1033 (1992).
[25] Walsh, J.M. and Gubbins, K.E., *Mol. Phys*., **80**, 65 (1993).
[26] NIST Chemistry WebBook, NIST Standard Reference Database, Number 69 (June 2005).